The Excess Heat Capacity in Glass-forming Liquid Systems Containing Molecules

ARTICLE *in* SCIENCE CHINA: PHYSICS, MECHANICS AND ASTRONOMY · NOVEMBER 2011

Impact Factor: 1.14 · DOI: 10.1007/s11433-013-5097-2 · Source: arXiv

3 AUTHORS, INCLUDING:

Hai Bo Ke
China Academy of Engineering Physics
17 PUBLICATIONS **150** CITATIONS
SEE PROFILE

Wei-Hua Wang
Chinese Academy of Sciences
434 PUBLICATIONS **12,294** CITATIONS
SEE PROFILE

SCIENCE CHINA
Physics, Mechanics & Astronomy

• Article •

June 2013 Vol.56 No.6: 1090–1095
doi: 10.1007/s11433-013-5097-2

Excess heat capacity in glass-forming liquid systems containing molecules

KE HaiBo, WEN Ping* & WANG WeiHua

Institute of Physics, Chinese Academy of Sciences, Beijing 100190, China

Received March 28, 2012; accepted April 26, 2012; published online May 3, 2013

Excess heat capacities at glass transition temperature in two types of glass-forming systems of $[x\mathrm{NaNO_3}\cdot(1-x)\mathrm{KNO_3}]_{60}\cdot[\mathrm{Ca(NO_3)_2}]_{40}$ ($0 \leqslant x \leqslant 1$) and $\mathrm{Ca(NO_3)_2}\cdot y\mathrm{H_2O}$ ($4 \leqslant y \leqslant 13$) are studied. In the former system, with the replacement of $\mathrm{K^+}$ cation with $\mathrm{Na^+}$ cation, the excess heat capacity is around 65.1 $\mathrm{J\cdot mol^{-1}\cdot K^{-1}}$, while the excess increases by 38.9 $\mathrm{J\cdot mol^{-1}\cdot K^{-1}}$ upon one molar $\mathrm{H_2O}$ content in latter system. A quantitative description to the excess heat capacity is built up with the thermal effects of atomic and molecular translational motion in liquids. The results might offer a further understanding to the glass transition.

glass-forming liquid, excess heat capacity, the glass transition

PACS number(s): 64.70.P-, 64.70.ph, 65.20.Jk

Citation: Ke H B, Wen P, Wang W H. Excess heat capacity in glass-forming liquid systems containing molecules. Sci China-Phys Mech Astron, 2013, 56: 1090–1095, doi: 10.1007/s11433-013-5097-2

1 Introduction

Excess heat capacity of glass forming liquids relative to their rigid glasses or crystalline materials is a main objective in statistical mechanical theories of glass transition [1–3], and of particular importance to the understanding of the mysterious glass transition [1,4]. For most glass-forming liquids, the excess heat capacity ΔC_P is well above zero, meaning that a nonzero temperature T_K called usually as Kauzmann temperature always exists to satisfy the equation,

$$\Delta S_\mathrm{f} = \int_{T_\mathrm{K}}^{T_\mathrm{m}} \frac{\Delta C_\mathrm{P}}{T}\mathrm{d}T,$$

where ΔS_f is the fusion entropy and T_m is the melting point. The entropy of a liquid would tend to be less than its crystals when temperature is below T_K and eventually become negative upon cooling. This situation is termed as Kauzmann's paradox [5], implying the glass transition as a kinetically controlled manifestation of an underlying thermodynamic transition to an ideal glass with a unique configuration [6]. Consistent with the connection between the kinetics and thermodynamics of the glass transition, the well-known entropy model [1,7] provides a conventional wisdom to the ΔC_P. The ΔC_P increases with decreasing temperature, and is larger at the glass transition temperature T_g for a more fragile glass forming liquid (GFL) [8]. The weakness of the conventional understanding to the ΔC_P is the fact that the concept of a cooperatively rearranging region is invoked. The cooperatively rearranging region containing at least two different configurational states and the corresponding entropy of liquids separated into a vibrational and configurational part can not be used to formulate the ΔC_P [9]. Moreover, there are many exceptions [10]. Currently the ΔC_P at T_g for a serial of bulk metallic glass formers is found to be independent of the fragility and close to a constant ($3R/2$, R is gas constant) [11]. In particular, it has been found that the ΔC_P of metallic $\mathrm{Pd_{40}Ni_{10}Cu_{30}P_{20}}$ glass

*Corresponding author (email: pwen@aphy.iphy.ac.cn)

liquid is of temperature-independence, and equal to 3*R*/2 [12].

The finding of the ΔC_P (3*R*/2) in bulk metallic glass liquids offers a deep understanding of the glass transition since it is intuitive and appropriate to connect the atomic translational motion with the ΔC_P. According to statistical physics, the contribution of the translational motion to heat capacity for one mole atoms can be given as 3*R*/2. The result indicates that the nature of the glass transition is directly related to the atomic translational motion in the bulk metallic forming liquids. A translational process activated thermally in a liquid needs overcome an energy barrier ΔE (see Figure 1). The averaged $\Delta\bar{E}$ arisen from the interactions between atoms in general depends on temperature at constant pressure because of the anharmonic effect. So the averaged structural relaxation time in a GFL still follows the general Arrhenius form:

$$\tau = \tau_0 \exp\left(\frac{\Delta \bar{E}(T)}{k_B T}\right).$$

Upon cooling, the dramatic increase in τ of most GFLs arises from the increase $\Delta E(T)$ relative to $k_B T$. As temperature is approaching to T_g, the large τ can be compared with the probing time. Further cooling will make τ larger than the probing time, then the structural relaxation/rearrangement can not be observed within the probing time, and glass is formed. However, the ΔC_P at T_g for GFLs with wide spectra has a wide distribution [4,12]. The molecular GFLs containing molecule with more complicated molecular structure have larger ΔC_P at T_g [13]. It is meaningful to investigate firstly the origin of ΔC_P of glass-forming liquids containing sample molecules.

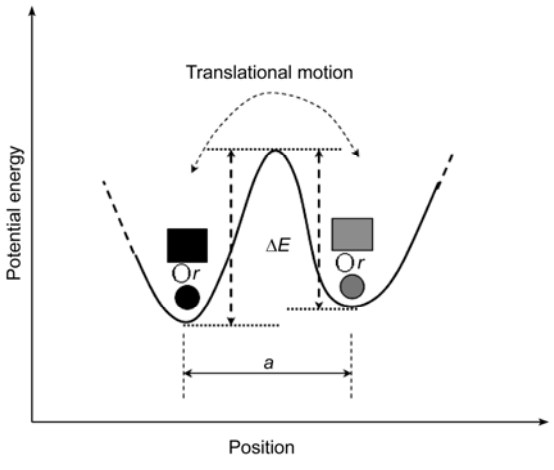

Figure 1 Schematic diagram for atomic (circle) or molecular (square) motions with their energy barrier (ΔE) to translational motion in a liquid. As the probing time is longer than the residual time τ ($\tau \simeq \tau_0 \exp[\Delta E/k_B T]$), the translational motion (jumping with a space (*a*) between atoms or molecules) can be observed. Conversely, atom or molecule only vibrates or oscillates around a fixed position.

2 Experimental

In this paper, two types of glass forming systems with the composition of $[x\mathrm{NaNO_3}\cdot(1-x)\mathrm{KNO_3}]_{60}\cdot[\mathrm{Ca(NO_3)_2}]_{40}$ ($0 \leqslant x \leqslant 1$) and $\mathrm{Ca(NO_3)_2}\cdot y\mathrm{H_2O}$ ($4 \leqslant y \leqslant 13$) are chosen. The two systems containing atomic ion and simple molecules ($\mathrm{NO_3^-}$ and $\mathrm{H_2O}$) with good glass-forming ability offer a good opportunity to understand further the origin of the ΔC_P for the GFLs. The materials were formed directly by the melting of mixtures of deionized water, $\mathrm{NaNO_3}$, $\mathrm{KNO_3}$, and $\mathrm{Ca(NO_3)_2}\cdot 4\mathrm{H_2O}$. Reagent grade $\mathrm{NaNO_3}$, $\mathrm{KNO_3}$, and $\mathrm{Ca(NO_3)_2}\cdot 4\mathrm{H_2O}$ are obtained from Sigma-Aldrich (USA), which are directly used without further purification. The detail preparation of $6[x\mathrm{NaNO_3}\cdot(1-x)\mathrm{KNO_3}]\cdot 4[\mathrm{Ca(NO_3)_2}]$ materials and samples used in the measurements of differential scanning calorimeter (DSC) has been reported previously [14]. The $\mathrm{Ca(NO_3)_2}\cdot y\mathrm{H_2O}$ materials with the mass of 5 g were sealed into glasses vials, which were held at 333 K for 30 min in order to homogenize the mixture. Thermal analysis occurring during both cooling and heating was carried out using a Mettler Toledo DSC1 thermal analyzer. The mass of the samples used for DSC measurements are around 15 mg. With the precise measurement, a correlation between the translational motion and the ΔC_P at T_g in the two GFL systems is built up. This result confirms further that the glass transition is directly related to the translational motion in GFLs.

3 Results and discussion

Figure 2 displays the DSC curves for the $[x\mathrm{NaNO_3}\cdot(1-x)\mathrm{KNO_3}]_{60}\cdot[\mathrm{Ca(NO_3)_2}]_{40}$ ($0 \leqslant x \leqslant 1$) materials. All of curves were measured at a heating rate of 20 K/min. The measurements followed a cooling from the temperature (T_g+20 K) at 20 K/min for each DSC sample. Potassium, sodium and calcium ions have spherical charge distributions, which are different from nitrate ions with trigonal shape. Thus the system can be regarded as a binary mixture. It has been reported that the glass-forming ability of $[x\mathrm{NaNO_3}\cdot(1-x)\mathrm{KNO_3}]_{60}\cdot[\mathrm{Ca(NO_3)_2}]_{40}$ ($0 \leqslant x \leqslant 1$) systems become worse with the increase of x [14]. Even so, a clear glass transition with an apparent ΔC_P and supercooled liquid region are still observed for all of samples with different compositions. The T_g determined by the usual way (see Figure 2) depends on the composition. With the replacement of the first alkali ionic (K^+) by the second alkali ionic Na^+, T_g decreases gradually to a minimum as x approaches to 0.5. A similar phenomenon has been found in the system representing the alkali-mixed effect [15]. The fragility index m of GFLs given by DSC measurements [14], T_g, and the ΔC_P at T_g for the system are listed in Table 1.

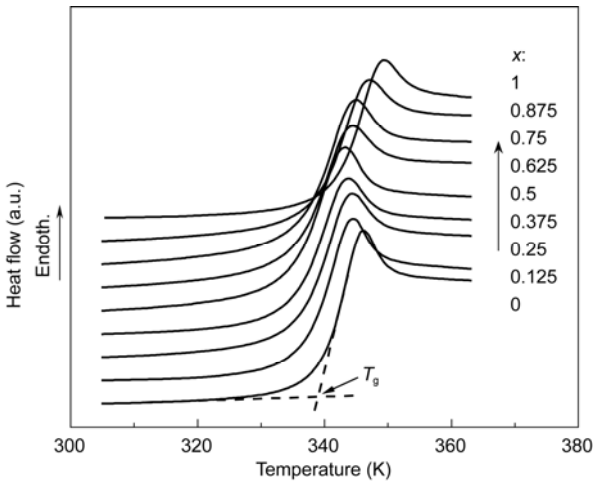

Figure 2 DSC curves of $[x\mathrm{NaNO_3}\cdot(1-x)\mathrm{KNO_3}]_{60}\cdot[\mathrm{Ca(NO_3)_2}]_{40}$ ($0 \leqslant x \leqslant 1$) glassy samples measured during a heating at 20 K/min.

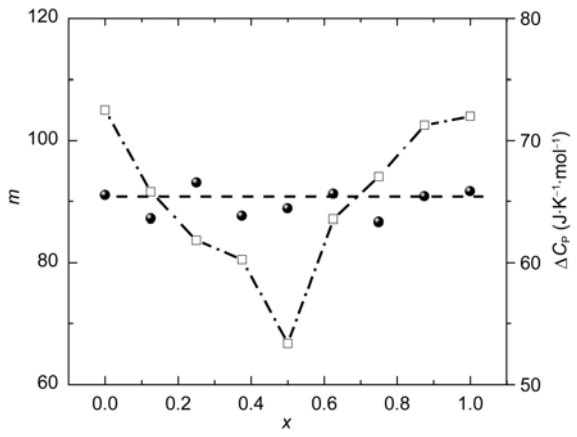

Figure 3 x dependence one the ΔC_p at T_g and the fragility index m for $[x\mathrm{NaNO_3}\cdot(1-x)\mathrm{KNO_3}]_{60}\cdot[\mathrm{Ca(NO_3)_2}]_{40}$ glass-forming system.

Figure 3 shows the x dependence of the fragility index m and the ΔC_P of the $[x\mathrm{NaNO_3}\cdot(1-x)\mathrm{KNO_3}]_{60}\cdot[\mathrm{Ca(NO_3)_2}]_{40}$ system. The value of m for the system depends on the composition. The tendency of m with x is similar to that of T_g. $[\mathrm{KNO_3}]_{60}[\mathrm{Ca(NO_3)_2}]_{40}$ with extreme $x = 0$ is termed usually as CKN, whose m is 107. As x tends to 0.5, m approaches to a minimum. In contrast, the ΔC_p is almost independent of the composition and close to a constant value of 65.2 $\mathrm{J\cdot K^{-1}\cdot mol^{-1}}$. This indicates that no relation between the ΔC_p and the m exists in this system. Therefore, the reputed understanding that GFLs with large m has a large ΔC_p at T_g [4,8] can not be applied in this GFL system.

The carriers of the motions in the system can be classified into two types: One contains $\mathrm{K^+}$, $\mathrm{Na^+}$, and $\mathrm{Ca^{2+}}$ ion, and another involves only $\mathrm{NO_3^-}$ ions. It is appropriate to think that the contributions of atomic ($\mathrm{K^+}$, $\mathrm{Na^+}$, and $\mathrm{Ca^{2+}}$) motion to the heat capacity are equivalent because the ΔC_p is invariable as $\mathrm{K^+}$ is replaced by $\mathrm{Na^+}$. The ΔC_p at T_g is then separated into two parts: cationic and anionic ones. Defining C_P^ca related to one mole cations and C_P^an for one mole anionic $\mathrm{NO_3^-}$, the ΔC_p in the system has the form as: $\Delta C_\mathrm{P} = C_\mathrm{P}^\mathrm{ca} + 1.4\cdot C_\mathrm{P}^\mathrm{an} = 64.9\ \mathrm{J\cdot K^{-1}\cdot mol^{-1}}$. To determine the values of the C_P^ca and C_P^an, another equation containing the C_P^ca and C_P^an must be provided.

Figure 4 shows the DSC curves for a series of $\mathrm{Ca(NO_3)_2}\cdot y\mathrm{H_2O}$ ($4 \leqslant y \leqslant 13$) samples. The values of T_g and the ΔC_p at T_g for all of materials are listed in Table 1. In this system, T_g decreases gradually with the increasing $\mathrm{H_2O}$ content, while the ΔC_p at T_g increases. The large value of ΔC_p at T_g for $\mathrm{Ca(NO_3)_2\cdot 4H_2O}$ (approximately 234.3 $\mathrm{J\cdot K^{-1}\cdot mol^{-1}}$) has been explained with its large m (~ 100) [13]. It is also contrary to the conventional wisdom since $\mathrm{Ca(NO_3)_2\cdot 4H_2O}$ GFL has much larger ΔC_p than CKN while its m is smaller than CKN. We think the key reason is that the particles involving $\mathrm{Ca^+}$, $\mathrm{NO_3^-}$, and $\mathrm{H_2O}$ in one molar $\mathrm{Ca(NO_3)_2\cdot 4H_2O}$ are more than those in one molar CKN.

Following the above description of the ΔC_p at T_g in $[x\mathrm{NaNO_3}\cdot(1-x)\mathrm{KNO_3}]_{60}\cdot[\mathrm{Ca(NO_3)_2}]_{40}$ system, the ΔC_p for $\mathrm{Ca(NO_3)_2}\cdot y\mathrm{H_2O}$ system is given as the form: $C_\mathrm{P}^\mathrm{ca} + 2\cdot C_\mathrm{P}^\mathrm{an} + y\cdot C_\mathrm{P}^{\mathrm{H_2O}}$, where $C_\mathrm{P}^{\mathrm{H_2O}}$ is related to one molar $\mathrm{H_2O}$ mole-

Table 1 The values of T_g, ΔC_P at T_g and m determined by DSC for the $\mathrm{Ca(NO_3)_2}\cdot y\mathrm{H_2O}$ and $[x\mathrm{NaNO_3}\cdot(1-x)\mathrm{KNO_3}]_{60}\cdot[\mathrm{Ca(NO_3)_2}]_{40}$ ($0 \leqslant x \leqslant 1$) materials

$\mathrm{Ca(NO_3)_2}\cdot y\mathrm{H_2O}$			$[x\mathrm{NaNO_3}\cdot(1-x)\mathrm{KNO_3}]_{60}\cdot[\mathrm{Ca(NO_3)_2}]_{40}$			
y	T_g (K)	ΔC_p ($\mathrm{J\cdot mol^{-1}\cdot K^{-1}}$)	x	T_g (K)	m	ΔC_p ($\mathrm{J\cdot mol^{-1}\cdot K^{-1}}$)
4	212	234.3	0	339	105	65.5
5	202	281.3	0.125	336	91.5	63.6
6	194	295.5	0.25	335	83.7	66.5
7	187	358.5	0.375	335	80.5	63.8
8	182	397.5	0.5	334	66.7	64.4
9	178	434.3	0.625	335	87.1	65.6
10	174	477.5	0.75	335	94	63.3
11	171	504.2	0.875	337	102.5	65.4
12	168	534.8	1	341	104	65.8
13	166	570.2	–	–	–	–

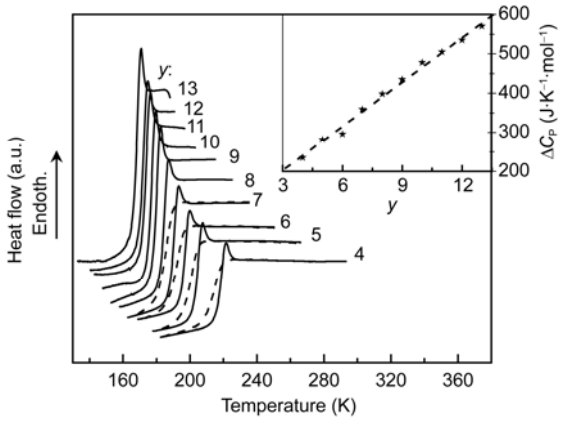

Figure 4 DSC curves for series of $Ca(NO_3)_2{\cdot}yH_2O$ ($4 \leqslant y \leqslant 13$) glassy samples measured during a heating at 20 K/min. The dash lines are the curves measured during a cooling at 10 K/min. The inset displays the linear relation between ΔC_p at T_g and y in $Ca(NO_3)_2{\cdot}yH_2O$ system. The slope of the fitting line is 37.8 $J{\cdot}mol^{-1}{\cdot}K^{-1}$, and interact on vertical axis is 87.6 $J{\cdot}mol^{-1}{\cdot}K^{-1}$.

cules. In the equation, the only variable is y that is H_2O mole content. If this description is accepted, it will be found that the change of ΔC_p in the system must be proportional to the change of y. Correspondingly, the values of the $C_P^{H_2O}$ and the sum $C_P^{ca}+2\cdot C_P^{an}$ can be deduced from the linear relation between the ΔC_p and y. The linear increase of the ΔC_p with the increase of y in the system is confirmed in the inset of Figure 4. The slope and the intercept on vertical axis of the linear relation are 37.9 and 87.6 $J{\cdot}mol^{-1}{\cdot}K^{-1}$, respectively. Thus, the values of $C_P^{H_2O}$ and $C_P^{ca}+2\cdot C_P^{an}$ are 37.9 and 87.6 $J{\cdot}mol^{-1}{\cdot}K^{-1}$. Combined with the above result: $C_P^{ca}+1.4\cdot C_P^{an}=64.9\ J\cdot K^{-1}\cdot mol^{-1}$, the resultant values of the C_P^{ca} and C_P^{an} are 12.0 and 37.8 $J{\cdot}mol^{-1}{\cdot}K^{-1}$. It is found remarkably that the value of the C_P^{ca}, C_P^{an} and $C_P^{H_2O}$ is close to $3R/2$ (approximately 12.5 $J{\cdot}mol^{-1}{\cdot}K^{-1}$), $9R/2$ (~37.4 $J{\cdot}mol^{-1}{\cdot}K^{-1}$) and $9R/2$ with a small reasonable error, respectively. These values have definitive physical meaning, implying that a certain type of motion in liquids is involved.

It is usual, in theoretical considerations, to ignore the difference between C_P at constant pressure and C_V at constant volume for a condensed matter. This neglect involves only small errors (appearing principally in the term of $TV\alpha^2/\beta$, α is the coefficient of linear expansion, β the compressibility and V the volume), and can be remedied. In theory, C_V can be calculated directly from the motions of particles, whose additive integrals completely define the statistical properties of a closed system [16]. The motions of particles in a liquid involve vibrations, rotations and translations. Clearly, atomic vibrations in the GFLs have no relation with C_P^{ca}. The vibrations for one atom with six degrees of freedom contribute $6k_B/2$ to heat capacity, and exist in both of glass and liquid. The remaining atomic motions, contributing to the C_P^{ca}, are only atomic translational motions. These motions are related to the atomic jumps away from their positions in the supercooled liquid state. In space, each atomic translational motion has three independent directions with the same possibility. Thus, this motion has three degrees of freedom. The corresponding heat capacity arisen from atomic translation is $3R/2$, and exactly equal to the experimental value of C_P^{ca}. It is not surprising to find that the C_P^{ca} is exactly equal to the ΔC_P at T_g in bulk metallic GFLs [11,12]. In nature, it is arisen from the atomic translational motion.

Compared to atomic motions, the motions of NO_3^- atomic group and H_2O molecule are a little complex. NO_3^- in liquid has not only vibration, but also rotation and translation. The vibration related to NO_3^- atomic group involves the vibration of the whole molecule and the atoms inside the atomic group. The former has six degrees of freedom, and the latter has twelve degrees of freedom. At high temperature the vibrations of one mole NO_3^- contribute $18R/2$ to heat capacity. So, the C_P^{an} ($9R/2$) has not relation with the vibration. The rotation of NO_3^-, involving the rotation of trigonal plate and the rolling of oxygen around nitrogen inside the atomic group, has three degrees of freedom totally, and can not contribute to C_P^{an}. The translation of one NO_3^- atomic group in liquid contributes $9k_B/2$ (k_B is Boltzmann constant) to heat capacity, but $3k_B/2$. It is known that the molecular rotation activated by thermal energy is easier than the translation in condensed state [17,18]. In other words, as shown in Figure 1, molecular rotation takes place in the potential well, then the translation follows. According to the equipartition theorem, it is reasonable to consider that one NO_3^- molecule has three different energy states with same energy level. This means that there are three NO_3^- molecular forms to move translationally in space (see Figure 1). Clearly, the number of molecular forms determined by the number of degrees of rotational freedom is different for different molecules. One NO_3^- atomic group with a given molecular form has three degrees of translational freedom. Thus, the translational motion of one NO_3^- atomic group contributes $9k_B/2$ to heat capacity, and correspondingly the contribution of translational motion for one mole NO_3^- to heat capacity is $9R/2$. It is found that the translational contribution of NO_3^- is precisely equal to the C_P^{an}. Similar as NO_3^- atomic group, the correlation between $C_P^{H_2O}$ and the translational motion of H_2O molecule also exists. One H_2O molecule, regarded as a rigid bent, has three degrees of rotational

freedom. Correspondingly, one H_2O molecule has three molecular forms to move translationally in liquid. The contribution of one mole H_2O molecular translational motion in liquid to heat capacity is equal to $9R/2$. It is consistent with $C_P^{H_2O}$.

The above treatment of the translational contribution is new definitely and reasonable since it is based on that GFLs have equilibrium state, and obey the additive integrals of motion, a basic principle in statistical physics. The basic principle has been applied well in a gas system, where the heat capacity is formulated by the thermal effect of vibration, rotation and translation. However, there is an obvious difference between a gas and a liquid. That is, no interactions between the carriers of the motion exist in a gas, but in a liquid. Correspondingly, in a probing time window translation and rotation in a gas take place individually and independently, even though both of them exist. The situation in a gas can not be described by Figure 1. Then the contribution of translational motion on heat capacity for a gas system in physical textbook can not be used directly to explain the thermal effect of translational motion in a liquid. Our way to treat the translational contribution in a liquid is based on the idea that the number of degrees of translational freedom for a given molecule in a space is fixed to be three. Importantly, the special situation of a molecule in a liquid shown in Figure 1 must be considered, where translation follows rotation.

The finding that the ΔC_P at T_g has a close relation with the translational motion in GFLs offers a clear picture to the glass transition in GFLs. Upon cooling (see Figure 3), across the glass transition the rapid decrease in heat capacity is accompanied by the gradual disappearance of excess heat capacity in the GFLs within the DSC experimental time scale. Correspondingly, the nature of the glass transition is a pure kinetic process, which corresponds to the disappearance of translational motion in the GFLs within the experimental time scale. This means that the Kauzmann's paradox [5] is not a problem at all. The gradual disappearance of translational motion can not be related to any thermodynamic phase transition. On the thermodynamic view, the supercooled GFLs close to T_g have no difference from their normal liquids. As shown in Figure 1, a liquid in whole liquid region can not support any shear within an experimental time scale, which is longer than the averaged structural relaxation/rearrangement time determined by translational motions. In a short moment atoms or molecules interacted with the neighbors can vibrate and rotate around fixed position as it were an atom or a molecule in the solid state. At the next moment with a certain wide gap in time to the previous moment, the atoms/molecules may already move translationally away from its previous site. The clarification of the ΔC_P at T_g indicates that it is not necessary to suppose the cooperative rearrangement region in order to understand the slowing down of GFLs upon cooling. It can be understood that the slowing down corresponds the change of activation energy (ΔE, see Figure 1) of translational motion relative to the thermal energy k_BT [4]. The ΔE depended on the complex interaction in the system and its distributions in GFLs are the key interest in the dynamics of the glass transition [19], and beyond the study here. Although the origin of the ΔC_P at T_g for the GFLs opens a fundamental understanding to the ΔC_P for all of GFLs with a wide spectra, future confirmations and breakthroughs are likely to come from careful and accurate experiments.

4 Conclusions

In summary, the clear correlation between the excess heat capacity and the atomic and molecular translational motion in $[x\mathrm{NaNO_3}\cdot(1-x)\mathrm{KNO_3}]_{60}\cdot[\mathrm{Ca(NO_3)_2}]_{40}$ $(0 \leqslant x \leqslant 1)$ and $\mathrm{Ca(NO_3)_2}\cdot y\mathrm{H_2O}$ $(4 \leqslant y \leqslant 13)$ glass-forming systems is built. The results show that within the DSC experimental time scale almost all of translational motions are available in supercooled liquids, but in their glasses. The glass transition in the two glass-forming systems is related to the frozen of translational motions in the GFLs.

This work was supported by the National Natural Science Foundation of China (Grant Nos. 51071170 and 11274353) and the National Basic Research Program of China (Grant Nos. 2007CB613904 and 2010CB-731603).

1 Gibbs J H, DiMarzio E A. Nature of the glass transition and the glassy state. J Chem Phys, 1958, 28: 373–383
2 Goldstain M. Viscous liquids and the glass transition. V. Sources of the excess specific heat of the liqiuid. J Chem Phys, 1976, 64: 4767–4773
3 Angell C A. Strong and fragile liquids. In: Ngai K L, Wright G B, eds. Relaxations in Complex Systems. Washington D. C.: U.S. GPO, 1985. 3–11
4 Dyre J C. The glass transition and elastic models of glass-forming liquids. Rev Mod Phys, 2006, 78: 953–972
5 Kauzmann W. The nature of the glassy state and the behavior of liquids at low temperatures. Chem Rev (Washington D. C.), 1948, 43: 219–256
6 Debenedetti P G, Stillinger F H. Supercooled liquids and the glass transition. Nature, 2001, 410: 259–267
7 Adam G, Gibbs J H. On the temperature dependence of cooperative relaxation properties in glass-forming liquids. J Chem Phys, 1965, 43: 139–146
8 Angell C A. Entropy and fragility in supercooling liquids. J Res Natl Inst Stand Technol, 1997, 102: 171–185
9 Jäckle J. Models of the glass transition. Rep Prog Phys, 1986, 49: 171–231
10 Tanaka H. Relation between thermodynamics and kinetics of glass-forming liquids. Phys Rev Lett, 2003, 90: 055701
11 Ke H B, Wen P, Zhao D Q, et al. Correlation between dynamic flow and thermodynamic glass transition in metallic glasses. Appl Phys Lett, 2010, 96: 251902
12 Ke H B, Zhao Z F, Wen P, et al. Specific heat in a typical metallic glass former. Chin Phys Lett, 2012, 29: 046402

13 Wang L M, Angell C A, Richert R. Fragility and thermodynamics in nonpolymeric glass-forming liquids. J Chem Phys, 2006, 125: 074505
14 Wen P, Harrowell P, Angell C A. Fast and slow components in the crystallization of a model multicomponent system, NaKCa(NO3): The role of composition fluctuations. J Phys Chem A, 2011, 115: 6260–6268
15 Komatsu T, Noguchi T. Heat capacity changes at the glass transition in mixed-alkali tellurite glasses. J Am Ceram Soc, 1997, 80: 1327–1332
16 Laudau L D, Lifshitz E M. Statistical Physics. Oxford: Butterworth-Heinemann, Linacre House, Jordan Hill, 1999
17 Pauling L. The structure and entropy of ice and of other crystals with some randomness of atomic arrangement. J Am Chem Soc, 1935, 57: 2680–2684
18 Shen T Y, Mitra S S, Prask H, et al. Order-disorder phenomenon in sodium nitrate studied by low-frequency Raman scattering. Phys Rev B, 1975, 12: 4530–4533
19 Donth E. The Glass Transition-Relaxation Dynamics in Liquid and Disordered Materials. Berlin: Springer-Verlag, 2001